

Supporting Information

Surface engineering of 2D CuFe-LDH/MoS₂ photocatalyst for improved hydrogen generation

Chandra Shobha Vennapoosa,^{a,b} Sandip Prabhakar Shelake,^{b,c} Bhavya Jaksani,^{a,b} Aparna Jamma^{a,b} B. Moses Abraham,^d Annadanam V. Sesa Sainath,^{b,c} Mohsen Ahmadipour,^e Ujjwal Pal^{*a,b}

^aDepartment of Energy & Environmental Engineering, CSIR-Indian Institute of Chemical Technology, Tarnaka, Hyderabad, Telangana-500007, India.

^bAcademy of Scientific & Innovative Research (AcSIR), Ghaziabad, Uttar Pradesh-201002, India.

^cPolymers and Functional Materials and Fluoro-Agrochemicals Department, CSIR-Indian Institute of Chemical Technology, Uppal Road, Hyderabad 500007, India.

^dDepartment of Chemical Engineering, Indian Institute of Technology Kanpur, Kanpur-208016, India.

^e Institute of Power Engineering, Universiti Tenaga Nasional, 43650 Serdang, Selangor.

*Corresponding author: Ujjwal Pal, Email: upal03@gmail.com ; ujjwalpal@iict.res.in

± These authors contributed equally

Table of content

Content		Page No.
Serial No	Content	
1	S1 Experimental details	2-6
	S1.1 Preparation of photocatalyst	2-3
	S1.2 Characterizations	3-4
	S1.3 Computational Details	4-5

	S1.4 Photoelectrochemical Measurements	5-5
	S1.5 Photocatalytic Hydrogen Evolution	5-6
	Table. S1 Photocatalytic H ₂ generation efficiency of the composites under visible light irradiation for 4 hrs.	6-7
	Table. S2 Comparative table of photocatalytic hydrogen evolution activity.	7-7
2	Figures	8-9
	Fig. S1 PXRD analysis of increased in the peak intensity of MoS ₂ .	8-8
	Fig. S2 HRTEM of the images of (a-b) MoS ₂ and (c) CuFe-LDH.	8-8
	Fig. S3 (a-b) The N ₂ adsorption-desorption isotherms of MoS ₂ , CuFe-LDH, and CuFe-LDH/MoS ₂ (20)	9-9
	Fig S4 High resolution XPS spectra of CuFe-LDH, MoS ₂ and CuFe-LDH/MoS ₂ : (a) C1s (b) N1s	9-9
	Fig: S5 Comparison of (a) XRD and (b) XPS after and before activity of HER CuFe-LDH/MoS ₂ (20).	9-10
3	References	10-11

1. S1. Experimental Section:

S1.1 Preparation of photocatalyst

Fabrication of MoS₂. The synthesis of MoS₂ began by using thiourea and Na₂MoO₄ as sources for sulfur and Mo, respectively. Initially, a mixture of Na₂MoO₄ and thiourea in a 1:5 molar ratio was prepared in a solution consisting of 20 mL of EtOH and 60 mL of distilled water. This solution underwent 30 minutes of ultrasonic treatment, followed by continuous stirring for an

additional 30 minutes at room temperature. Subsequently, the resulting mixture was moved to a Teflon-lined stainless-steel autoclave and subjected to hydrothermal treatment at 210 °C for 24 hours. After the hydrothermal treatment, the autoclave was allowed to cool naturally to room temperature, leading to the formation of a black-colored precipitate. This precipitate was isolated through centrifugation at 6500 rpm and washed three times with EtOH and distilled water. The resulting product consisted of hexagonal sheet-like MoS₂ material, which was further dried in an oven at 80 °C for 12 hours to obtain the final composite.¹

Synthesis of the CuFe-LDH/MoS₂ nanocomposite. In a conventional procedure, the predetermined quantity of a metal salt solution containing [Cu]²⁺ and [Fe]³⁺ ions in a molar ratio of 5:1 was dissolved in 20 mL of double-distilled water.¹ Ultrasonic treatment for 30 minutes resulted in the formation of a clear solution containing metal nitrates. Subsequently, a 10 mL aqueous solution of NaOH (weighing 5.072 g) was slowly added to the metal salt solution, drop by drop, till the pH of the solution steadied at 9. The resulting product, denoted as CuFe-LDH gel (yielding approximately 2 grams), was dispersed in a mixed solvent comprising 75 mL of EtOH and 25 mL of H₂O, making the entire volume 100 mL, for a duration of 30 minutes. In a separate container, a predetermined quantity of Na₂MoO₄ and thiourea, in a 1:5 molar ratio, was subjected to sonication for 30 minutes in a solution containing 20 mL of EtOH and 60 mL of distilled H₂O. Subsequently, this MoS₂ precursor suspension was added drop wise to the clear gel dispersion of CuFe-LDH, while maintaining continuous stirring. The resulting mixture was further stirred for an additional hour to maintain electrostatic equilibrium. At this stage, the MoS₂ precursor was deposited onto the surface of the CuFe-LDH gel to form a composite mixture. This mixture was then transferred to a 100 mL Teflon autoclave and subjected to hydrothermal treatment at 210 °C for 24 hours. After cooling the Teflon container, the product was gained through centrifugation. The final composite was gained by washing with EtOH and deionized H₂O, followed by drying at 60 °C in vacuum. A series of electrostatic CuFe-LDH/MoS₂ composites were prepared by varying the wt.% of the MoS₂ precursor, specifically at 5%, 10%, 20%, and 30% with respect to CuFe LDH. These nanocomposites were denoted as CuFe-LDH/MoS₂-x, where x represents the weight percentage of MoS₂ against CuFe LDH, with values of 5, 10, 20, and 30.

S1.2 Characterization

The structural phase analysis of the as-synthesized photocatalysts was performed by using Powder X-ray diffraction patterns (XRD) on a Bruker AXS diffractometer (D8 advance) at a generator voltage of 40 kV and current of 30 mA using Cu-K α 1 irradiation ($\lambda = 1.5406 \text{ \AA}$). The sample was scanned in the range of $2\theta = 10\text{-}80^\circ$ with a scan rate of 1 s/step. X-ray photoelectron spectroscopy (XPS) was performed via a Kratos (axis 165) analytical instrument with Mg K α irradiation. About 10^{-9} Torr pressure was maintained in the spectrometer. The structural morphology of the photocatalysts was examined by using MIRA3 FEG-SEM (TESCAN) Scanning electron microscopy (SEM) at an accelerating voltage of 5 kV. Transmission electron microscopy (TEM) image of the representative photocatalysts was obtained by using a JEOL 2010EX TEM instrument equipped with the high-resolution style objective-lens pole piece at an acceleration voltage of 200 kV fitted with a CCD camera. N₂ adsorption-desorption isotherms of the photocatalysts were obtained on a Quanta chrome Nova 2200e gas adsorption analyzer at 77 K. The optical properties were characterized by using UV-Vis diffuse reflectance spectroscopy (DRS) Perkin Elmer Lambda 750 instrument using BaSO₄ as a reference. The sample has been placed in the sample holder for the measurement and the light is allowed to pass through the sample which leads to the absorption of the light and the light transmitted by the sample has been recorded. The Photoluminescence (PL) spectra were recorded using a Fluorolog-3 spectrofluorometer (Sp_{ex} model, JobinYvon) at their respective excitation (λ_{ex}) wavelength. Fluorescence Lifetime decay measurements were carried out by using time-correlated single-photon counting (TCSPC) setup (Fluorolog-3 Triple Illuminator, IBH Horiba Jobin Yvon). Briefly, the samples were excited at 380 nm, and the emission was observed at 434 nm.

S1.3 Computational details:

Periodic DFT calculations were performed with a plane-wave basis set to understand the enhanced photocatalytic activities of the MoS₂/CuFe-LDH using Vienna ab initio simulation package², where the interaction between the core and valence electrons are described via frozen-core projector augmented wave (PAW) method. The electronic structures of materials were described by Perdew–Burke–Ernzerhof (PBE) functional within the generalized gradient approximation (GGA), incorporating the treatment of long-range van der Waals interactions between layers in the heterostructure via the DFT-D3 dispersion correction method. A 20 Å

vacuum space is employed to mitigate interactions between adjacent layers along the $c(z)$ direction. A cutoff energy of 500 eV was selected for the plane-wave expansion, and precise convergence thresholds were implemented, specifying the self-consistent total-energy difference and atomic forces to be within the limit of 10^{-5} eV and 0.02 eV/Å, respectively. The Monkhorst-Pack method was employed to sample the Brillouin zone, utilizing a $5 \times 5 \times 1$ k-point mesh. The methodology for computing the Gibbs free energy of hydrogen adsorption (ΔG_H) can be found in our previous studies.³ To determine the transition state for water dissociation, we applied the nudged elastic band method. The structural optimization was accomplished by employing the conjugate-gradient algorithm, a method known for its efficiency in fine-tuning atomic arrangements and achieving energy minima in the system.

S1.4 Photo-electrochemical studies

The entire photo-electrochemical test was carried out in the electrochemical workstation. 0.25 M aqueous solution of Na_2SO_4 was used as an electrolyte for all experiments. Pt wire and calomel electrodes were used as counter and reference electrodes. The preparation of the working electrode is carried out using 20 μL of suspension (5 mg in 1mL ethanol) on ITO coated glass surface with a specific area of 2 cm^2 . The light source is considered as a photoelectrochemical measurement at room temperature were recorded on the CH Instruments Inc., USA, CHI6005E, Electrochemical Workstation with Potentiostat using a three-electrode system with a standard three-electrode system with the photocatalyst-coated ITO as the working electrode, Pt wire as the counter electrode, Ag/AgCl electrode as the reference electrode. The artificial solar simulator of AM 1G illuminator (100 mW cm^{-2}) was used as the light source during the measurement. The electrochemical cell was a conventional 7 three-electrode cell with a 3 mm thick Pyrex glass eyelet. A 0.25 M Na_2SO_4 solution was used as the electrolyte.

Electrode Preparation: To prepare the photo electrode, 4 mg of each as-synthesized photocatalyst was dispersed into a suspension that contained 0.3 ml ethanol and 40 μmol Nafion by 30 min of ultrasonication. The as-prepared solution was dropped on the surface of Indium tin oxide (ITO) film of $2 \times 2 \text{ cm}^2$ surface area to achieve uniform coverage and then dried in air at room temperature

S1.5 Photocatalytic Hydrogen Production

The photocatalytic hydrogen production by the water-splitting activity of MoS₂, CuFe-LDH, and CuFe-LDH/MoS₂ was investigated in a long-necked round bottom flask sealed with rubber septum in a nitrogen atmosphere at normal temperature and pressure. All samples were analyzed in the same reaction condition. Over a typical experiment, 10 mg of catalyst was dispersed in 40mL of aqueous Na₂S and Na₂SO₃ solution by ultrasonication. Before the irradiation reactor was evacuated, nitrogen was purged in dispersion to ensure a complete nitrogen atmosphere. The suspension was stirred continuously for homogeneous distribution of the catalyst. 420W Xe lamp was used as a light source for the water-splitting reaction. A 100μL airtight gas syringe was used to take outgas from the reactor. The resultant gases evolved through the reaction using a gas chromatograph equipped with Thermal Conductivity Detector (TCD). The apparent quantum efficiency (AQY) was calculated at wavelength 400nm ($\lambda_{\max} \pm 400\text{nm}$) using a UV-vis cutoff filter. The experimental conditions of our work are considered, and we tend to use an optical power meter (Newport, Model: 842-PE). The AQY (%) and the values of the Number of incident photons (N_{photons}) were calculated using the following equations:

$$N_{\text{photon}} = \frac{P\lambda t}{hc}$$

Here, P = power of light (0.19 J s⁻¹ cm⁻²) over a specific area of 12.26 cm², λ = light wavelength (420 nm), t = irradiation time (4 h), h - Planck's constant (6.626 x 10⁻³⁴ J s) and c = velocity of light (3 x 10⁸ m s⁻¹).

$$\text{AQY \%} = \frac{2 \times \text{the no. of evolved } H_2 \text{ molecule}}{\text{the no. of incident photons } (N_{\text{photon}})} \times 10$$

Table. S1 Photocatalytic H₂ generation efficiency of the composites under visible light irradiation for 4 hrs

Entry	Photocatalyst	Time (hrs)	Sacrificial agent	H ₂ activity (mmolg ⁻¹ h ⁻¹)	AQY (%)
1	CuFe-LDH	4	Na ₂ S /Na ₂ SO ₃	1.3	0.5%

2	MoS ₂	4	Na ₂ S /Na ₂ SO ₃	0.6	0.2%
3	CuFe-LDH/MoS ₂ (5)	4	Na ₂ S /Na ₂ SO ₃	1.5	0.6%
4	CuFe-LDH/MoS ₂ (10)	4	Na ₂ S /Na ₂ SO ₃	1.9	0.7%
5	CuFe-LDH/MoS₂(20)	4	Na₂S /Na₂SO₃	3.4	1.3%
6	CuFe-LDH/MoS ₂ (30)	4	Na ₂ S /Na ₂ SO ₃	2.4	0.9%

Table. S2 Comparative table of photocatalytic hydrogen evolution activity.

Entr y	Composite name	H₂ evolution rate (mmolg⁻¹h⁻¹)	Sacrificial agent	Reference s
1	NiAl-LDH/MoS ₂	4.5	TEOA	4
2	CoAl-LDH/MoS ₂	0.9	MeOH	5
2	NiFe LDH/N-rGO/g-C ₃ N ₄	2.50	NaNO ₂	6
3	g-C ₃ N ₄ /NiFe-LDH	1.48	CH ₃ OH/ NaNO ₂	7
4	MoS ₂ /NiFe-LDH	0.5	MeOH	8
5	NiFe-LDH/Zn _{0.5} Cd _{0.5} S	1.02	Lactic acid	9
6	ZIF-67/NiFe-LDH	0.11	TEOA	10
7	MOS ₂ /CdS	10.66	Lactic acid	11
10	CdS/Cu ₇ S ₄ /g-C ₃ N ₄	0.60	Na ₂ S /Na ₂ SO ₃	12
11	CuCdCe-LDH/ g-C ₃ N ₄	1.52	Na ₂ S /Na ₂ SO ₃	13
13	ZIF-67/CuFe-LDH	7.4	Na ₂ S /Na ₂ SO ₃	14
14	CuFe-LDH/MoS₂(20)	3.4	Na₂S /Na₂SO₃	This work

2. Figures

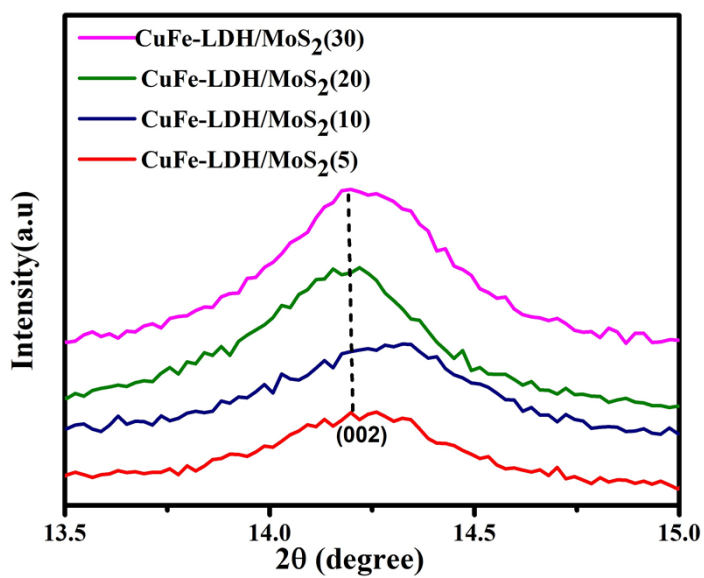


Fig. S1 PXRD analysis of increased in the peak intensity of MoS₂.

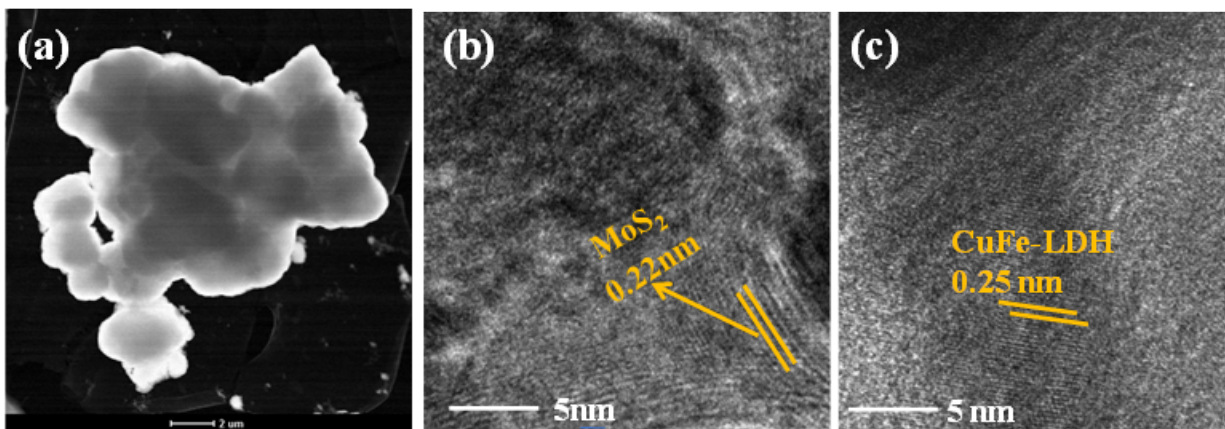


Fig.S2. HRTEM of the images of (a-b) MoS₂ and (c) CuFe-LDH.

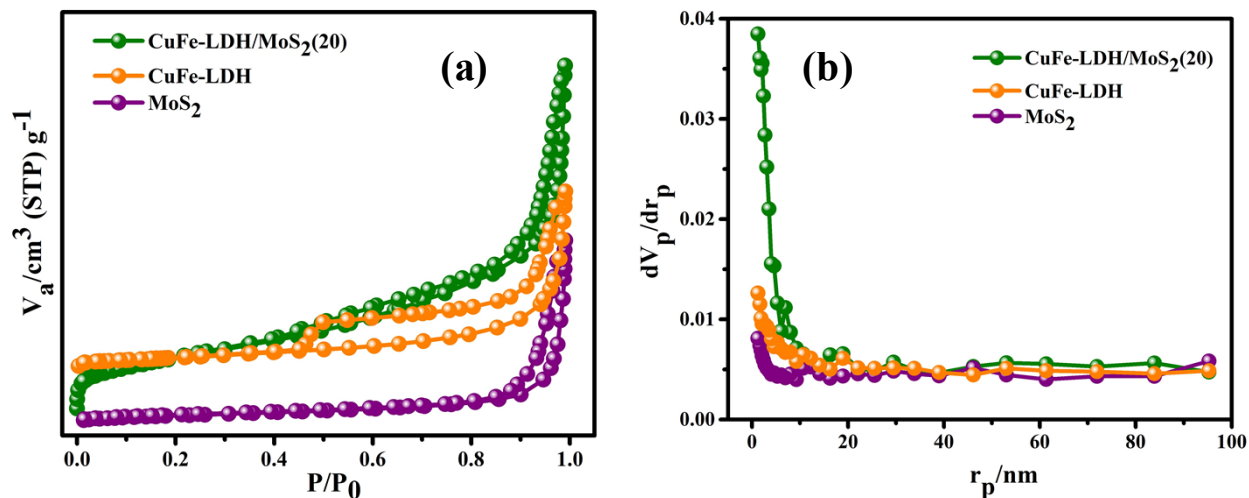


Fig. S3 (a-b) The N₂ adsorption-desorption isotherms of MoS₂, CuFe-LDH, and CuFe-LDH/MoS₂(20)

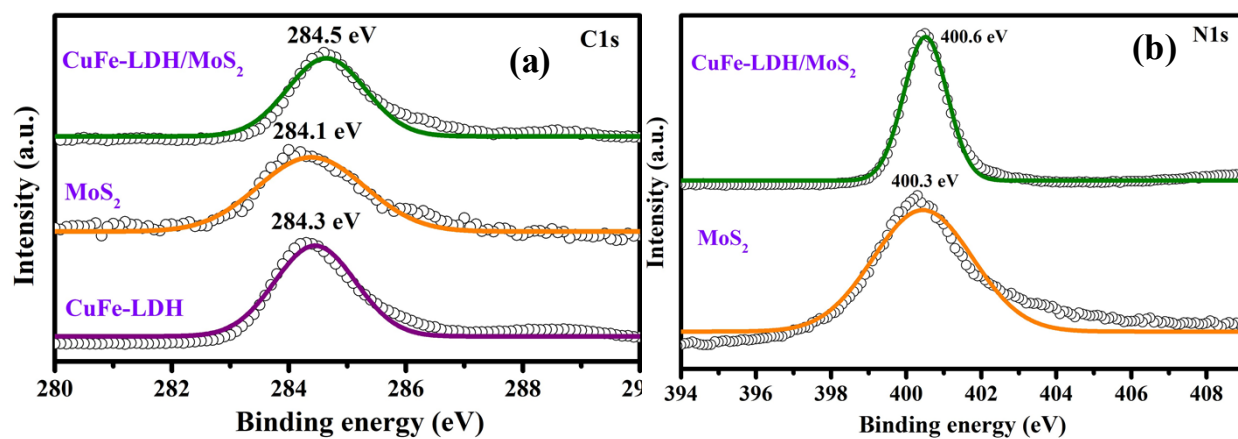


Fig. S4 High resolution XPS spectra of CuFe-LDH, MoS₂ and CuFe-LDH/MoS₂:(a) C1s (b) N1s.

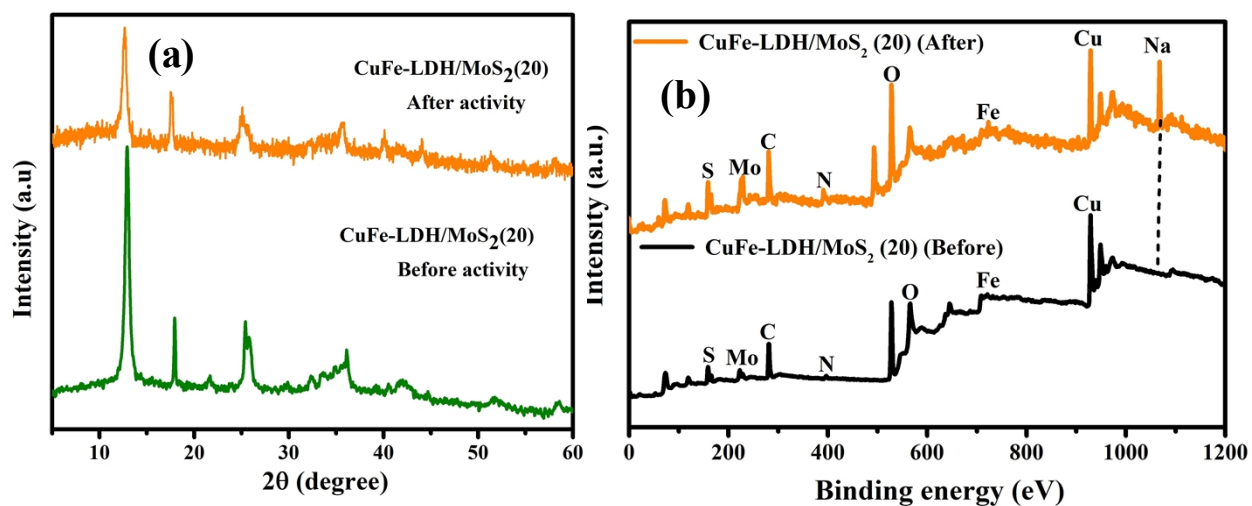


Fig: S5 Comparison of (a) XRD and (b) XPS after and before activity of HER CuFe-LDH/MoS₂ (20).

References

1. S. Nayak, G.; Swain, K. Parida, Enhanced Photocatalytic Activities of RhB Degradation and H₂ Evolution from in Situ Formation of the Electrostatic Heterostructure MoS₂/NiFe LDH Nanocomposite through the Z-Scheme Mechanism via p–n Heterojunctions,. *ACS Appl. Mater. Interfaces*, 2019, **11**, 20923–20942.
2. G. Kresse, J. Furthmuller, Efficient iterative schemes for *ab initio* total-energy calculations using a plane-wave basis set, *Phys. Rev. B: Condens. Matter Mater. Phys*, 1996, **54**, 11169-11186.
3. J. Heyd, G.E. Scuseria, Assessment and validation of a screened Coulomb hybrid density functional, *J. Chem. Phys*, 2004, **120**, 7274-7280.
4. X. Liu, J. Xu, L. Ma, Y. Liua, L. Hua Nano-flower S-scheme heterojunction NiAl-LDH/MoS₂ for enhancing photocatalytic hydrogen production, *New J. Chem*, 2022, **46**, 228-238.
5. J. Tao, X. Yu, Q. Liu, G. Liu, Tang, H. Internal Electric Field Induced S–scheme Heterojunction MoS₂/CoAl LDH for Enhanced Photocatalytic Hydrogen Evolution, *J. Colloid Interface Sci*, 2021, **585**, 470-479.
6. S. Nayak, K. Parida, Deciphering Z-scheme Charge Transfer Dynamics in Heterostructure NiFe-LDH/NrGO/g-C₃N₄ Nanocomposite for Photocatalytic Pollutant Removal and Water Splitting Reactions, *Sci. Rep*, 2019, **2458**, 1-23.
7. S. Nayak, L. Mohapatra, K. Parida, Visible light-driven novel g-C₃N₄/NiFe-LDH composite photocatalyst with enhanced photocatalytic activity towards water oxidation and reduction reaction, *J. Mater. Chem. A*, 2015, **3**, 18622-18635.
8. S. Nayak, G. Swain, K. Parida, Enhanced Photocatalytic Activities of RhB Degradation and H₂ Evolution from in Situ Formation of the Electrostatic Heterostructure MoS₂/NiFe LDH Nanocomposite through the Z-Scheme Mechanism via p–n Heterojunctions, *ACS Appl. Mater. Interfaces*, 2019, **11**, 20923–20942.
9. Y. Sun, X. Wang, Q. Fu, C. Pan, Construction of Direct Z-Scheme Heterojunction NiFe-Layered Double Hydroxide (LDH)/Zn_{0.5}Cd_{0.5}S for Photocatalytic H₂ Evolution, *ACS Appl. Mater. Interfaces*, 2021, **13**, 39331-39340.

10. K. Wang, S. Liu, P. Zhu, M. Yang, Z. Jin, Rational Design of a Novel S-Scheme Heterojunction based on ZIF-67-Supported Ni-Fe Layered Double Hydroxide for Efficient Photocatalytic Hydrogen Generation, *Energy Fuels*, 2022, **36**, 2058-2067.
11. X.L. Yin, L.L. Li, W.J. Jiang, Y. Zhang, X. Zhang, L.J. Wan, J.S. Hu, MoS₂/CdS Nanosheets-On-Nanorod Heterostructure for Highly Efficient Photocatalytic H₂ Generation under Visible Light Irradiation, *ACS Appl. Mater. Interfaces*, 2016, **8**, 15258–15266.
12. J. Chu, X. Han, Z. Yu, Y. Du, B. Song, P. Xu, Highly Efficient Visible-Light-Driven Photocatalytic Hydrogen Production on CdS/Cu₇S₄/g-C₃N₄ Ternary Heterostructures. *ACS Appl. Mater. Interfaces*, 2018, **10**, 20404–20411.
13. C.S. Vennapoosa, S. Varangane, B.M. Abraham, V. Perupogu, S. Bojja, U. Pal, Controlled photoinduced electron transfer from g-C₃N₄ to CuCdCe-LDH for efficient visible light hydrogen evolution reaction, *Int. J. Hydrog. Energy*, 2022, **47**, 40227-40241.
14. C.S. Vennapoosa, S. Varangane, S. Gonuguntla, B.M. Abraham, M. Ahmadipour, U. Pal. S-Scheme ZIF-67/CuFe-LDH Heterojunction for High-Performance Photocatalytic H₂ Evolution and CO₂ to MeOH Production. *Inorg. Chem*, 2023, **62**, 16451-16463.